The SPARC Intercomparison of Middle-Atmosphere Climatologies

WILLIAM RANDEL,[a] PETRA UDELHOFEN,[b] ERIC FLEMING,[c] MARVIN GELLER,[b] MEL GELMAN,[d] KEVIN HAMILTON,[e] DAVID KAROLY,[f] DAVE ORTLAND,[g] STEVE PAWSON,[c] RICHARD SWINBANK,[h] FEI WU,[a] MARK BALDWIN,[g] MARIE-LISE CHANIN,[i] PHILIPPE KECKHUT,[i] KARIN LABITZKE,[j] ELLIS REMSBERG,[k] ADRIAN SIMMONS,[l] AND DONG WU[m]

[a]*National Center for Atmospheric Research, Boulder, Colorado*
[b]*State University of New York at Stony Brook, Stony Brook, New York*
[c]*NASA Goddard Space Flight Center, Greenbelt, Maryland*
[d]*National Centers for Environmental Prediction, Washington, D.C.*
[e]*International Pacific Research Center, Honolulu, Hawaii*
[f]*University of Oklahoma, Norman, Oklahoma*
[g]*Northwest Research Associates, Bellevue, Washington*
[h]*Met Office, Exeter, United Kingdom*
[i]*Service d'Aeronomie, Paris, France*
[j]*Free University of Berlin, Berlin, Germany*
[k]*NASA Langley Research Center, Hampton, Virginia*
[l]*European Centre for Medium-Range Weather Forecasts, Reading, United Kingdom*
[m]*Jet Propulsion Laboratory, Pasadena, California*

(Manuscript received 30 April 2003, in final form 11 September 2003)

ABSTRACT

An updated assessment of uncertainties in ''observed'' climatological winds and temperatures in the middle atmosphere (over altitudes ~10–80 km) is provided by detailed intercomparisons of contemporary and historic datasets. These datasets include global meteorological analyses and assimilations, climatologies derived from research satellite measurements, historical reference atmosphere circulation statistics, rocketsonde wind and temperature data, and lidar temperature measurements. The comparisons focus on a few basic circulation statistics (temperatures and zonal winds), with special attention given to tropical variability. Notable differences are found between analyses for temperatures near the tropical tropopause and polar lower stratosphere, temperatures near the global stratopause, and zonal winds throughout the Tropics. Comparisons of historical reference atmosphere and rocketsonde temperatures with more recent global analyses show the influence of decadal-scale cooling of the stratosphere and mesosphere. Detailed comparisons of the tropical semiannual oscillation (SAO) and quasi-biennial oscillation (QBO) show large differences in amplitude between analyses; recent data assimilation schemes show the best agreement with equatorial radiosonde, rocket, and satellite data.

1. Introduction

Climatological datasets for the middle atmosphere are useful for empirical studies of climate and variability, and are also necessary for constraining the behavior of numerical models. Current general circulation model (GCM) simulations routinely extend into the middle atmosphere (model tops at 50 km or higher), and require observational datasets for validation (e.g., Pawson et al. 2000). A number of middle-atmosphere climatologies have been developed in the research community over the years, based on a variety of data sources and analysis techniques, and there are differences among these climatologies due to a number of reasons. For instance, the datasets are based on different combinations of radiosonde wind and temperature measurements and satellite temperature data, and global analyses are based on a variety of objective statistical analyses and data assimilation techniques. Also, the existence of strong decadal-scale trends in the stratosphere (Ramaswamy et al. 2001) means that a stratospheric climatology is itself time varying.

The earliest comprehensive climatologies for the middle atmosphere were the 1964 and 1972 Committee on Space Research (COSPAR) Reference Atmospheres (CIRA), which were based largely on interpolation of single-station balloon and rocket data. An updated version of CIRA in 1986 included early satellite observations of the stratosphere and mesosphere and has served as a community standard since that time. Daily meteorological analyses with significant stratospheric

Corresponding author address: Dr. William Randel, National Center for Atmospheric Research, P.O. Box 3000, Boulder, CO 80309-3000.
E-mail: randel@ucar.edu

coverage, which included operational satellite temperature soundings, began around 1979, and more recently (~1991) sophisticated model-based data assimilation schemes began to produce stratospheric analyses. These analyses (supplemented more recently by extensive retrospective reanalyses) have served as the basis for some more recent middle-atmosphere climatologies. Also, satellite observations from the *Upper-Atmosphere Research Satellite* (*UARS*; launched in 1991 and continuing to operate in 2003) have provided additional climatological datasets for the middle atmosphere. The circulation statistics derived from these various datasets will depend on several factors, including details of data inclusion and analysis techniques, and the respective time periods covered.

The scientific questions regarding middle-atmosphere climatological datasets have been studied by a Stratosphere Reference Climatology Group, under the auspices of the World Climate Research Programme (WCRP) Stratospheric Processes and Their Role in Climate (SPARC) project. To evaluate current understanding and uncertainties, this group decided that two valuable contributions would be to 1) bring together climatological datasets currently in use and make them available to the broader research community, and 2) make detailed intercomparisons of these datasets to highlight biases and uncertainties. The SPARC Data Center (information available online at http://www.sparc.sunysb.edu) was established partially in response to the first contribution, and an extensive technical report of intercomparisons was compiled in response to the second contribution (SPARC 2002). This paper includes a summary of the intercomparisons in that report, with further emphasis on assessing current uncertainties.

The analyses presented here bring together several middle-atmosphere climatological datasets that are in current use in the research community, and make direct comparisons of some basic measured and derived quantities. The climatologies include those derived from global meteorological analyses and satellite data, plus results from two independent datasets: historical rocketsonde wind and temperature measurements (covering 1970–89), plus lidar temperature data (covering the 1990s). The comparisons are used to identify biases in particular datasets, and also to highlight regions where there is relatively large uncertainty for particular quantities (i.e., where large differences are found among several datasets). Where possible, we provide some brief explanations as to why there are uncertainties and/or why the datasets might differ. However, more in-depth and detailed explanations are beyond the scope of this paper.

All of the monthly mean data presented and compared here are available to the research community via the SPARC Data Center (online at http://www.sparc.sunysb.edu). This paper and the more extensive SPARC (2002) report are intended to be companions to those online data.

2. Climatological datasets for the middle atmosphere

a. Description of global analyses

Two fundamental types of observations contribute to global (or hemispheric) stratospheric analyses. Radiosondes provide vertical profiles of temperature, pressure, and horizontal winds, covering the lowest 20–30 km of the atmosphere. The current radiosonde network provides approximately ~1100–1200 soundings per day, almost evenly split between measurements at 0000 and 1200 UTC; the vast majority of stations are located over landmasses of the Northern Hemisphere (NH). Almost all of these soundings (>1000) reach at least 100 hPa, with ~800 reaching 30 hPa and ~350 reaching up to 10 hPa. Satellite-derived temperature profiles are the other major source of stratospheric data. Operational meteorological polar-orbiting satellites provide near-global temperature profile retrievals twice daily up to ~50 km altitude, but have the drawback of relatively low vertical resolution (>10 km) in the stratosphere. A series of operational National Oceanic and Atmospheric Administration (NOAA) satellites has been in orbit since late 1978, containing a suite of instruments that are collectively called the Television Infrared Observation Satellite (TIROS) Operational Vertical Sounder (TOVS; Smith et al. 1979). An improved set of temperature and humidity sounders [called the Advanced TOVS (ATOVS)] is now replacing the older TOVS series, beginning with the *NOAA-15* satellite launched in May 1998.

Details of the various stratospheric analyses are described below, but the types of global or hemispheric analyses can be summarized as follows (acronyms defined in Table 1). The most straightforward analyses provide global or hemispheric fields based on hand-drawn analyses (FUB) or objective analysis gridding techniques (CPC and UKTOVS). More sophisticated analyses can be derived by the use of numerical forecast models to predict first-guess fields, and incorporate observations by optimal data assimilation (METO, NCEP, ERA-15, and ERA-40 data). Most of the analyses discussed below are based on very similar radiosonde and satellite data, and so the differences revealed in our comparisons highlight the sensitivity of the final statistics to details of the data usage and analysis techniques.

In the following we present short descriptions of the global datasets included in the comparisons. These are intended to be brief, and more details for each analysis can be found in the listed references. Table 1 provides a summary list of some relevant details for each analysis, including the acronyms used here.

TABLE 1. Middle atmosphere datasets included in the SPARC intercomparisons.

Data source	Acronym	Reference	Type of analysis	Time period available
Met Office stratospheric analyses	METO	Swinbank and O'Neill (1994)	Assimilation	Nov 1991–present
Met Office TOVS analyses	UKTOVS	Bailey et al. (1993)	Objective analysis	Jan 1979–Apr 1997
National Centers for Environmental Prediction (NCEP) Climate Prediction Center	CPC	Gelman et al. (1986)	Objective analysis (above 100 hPa)	Oct 1978–present
NCEP–National Center for Atmospheric Research (NCAR) reanalysis	NCEP	Kalnay et al. (1996)	Assimilation	1957–present
15-yr European Centre for Medium-Range Weather Forecasts (ECMWF) reanalysis	ERA-15	Gibson et al. (1997)	Assimilation	1979–93
40-yr ERA	ERA-40		Assimilation	1957–2002
Free University of Berlin stratospheric analyses	FUB	Labitzke et al. (2002)	Historical analysis (NH only)	1957–2001
1986 CIRA	CIRA86	Fleming et al. (1990)	Various	Various (1960s–1970s)
Halogen Occultation Experiment (HALOE) temperatures	HALOE	Russell et al. (1993)	Harmonic analysis of seasonal cycle	1992–2001
Microwave Limb Sounder temperatures	MLS	Wu et al. (2002)	Harmonic analysis of seasonal cycle	Jan 1992–Dec 1994
UARS Reference Atmosphere Program zonal winds	URAP	Swinbank and Ortland (2002)	METO and HRDI data	Jan 1992–Dec 1998

1) METO

Since October 1991 stratospheric analyses have been produced daily using a stratosphere–troposphere version of the Met Office's data assimilation system (Swinbank and O'Neill 1994). These analyses were formerly referred to as the UK Meteorological Office (UKMO) stratospheric analyses, but are referred to here as METO. The analyses consist of temperatures, wind components, and geopotential heights on a global grid of resolution 2.5° latitude × 3.75° longitude, output on the UARS standard pressure levels (with six equally spaced levels per decade of pressure). The analyses span the range 1000–0.3 hPa (approximately 0–55 km).

The stratospheric analyses were originally produced as correlative data for the National Aeronautics and Space Administration (NASA) UARS project, starting in October 1991. Since October 1995 the separate UARS assimilation system was discontinued, but stratospheric analyses continue to be produced using a similar data assimilation system, which is run as part of the Met Office operational forecasting suite. Since November 2000 the Met Office stratospheric analyses have been produced using a new three-dimensional variational data assimilation (3DVAR) system (Lorenc et al. 2000).

2) UKTOVS

The Met Office also produced objective stratospheric analyses (not part of a model assimilation) from measurements made by NOAA operational satellites. These analyses are referred to as UKTOVS. Monthly means from these analyses are available for the period January 1979–April 1997. The analysis method is described by Bailey et al. (1993), and Scaife et al. (2000) present climatological data and interannual variations diagnosed from the UKTOVS data.

The UKTOVS fields are derived from an independent analysis of TOVS radiance measurements. The daily TOVS data were used to derive geopotential thickness values, covering the layers 100–20, 100–10, 100–5, 100–2, and 100–1 hPa. The thicknesses were then mapped onto a 5° resolution global grid, and added to the operational analysis of 100-hPa height (obtained from Met Office operational global analyses) to produce height fields up to 1 hPa. In turn, temperatures and horizontally balanced winds are derived from the height fields.

3) CPC

Operational daily analyses of stratospheric geopotential height and temperature fields have been produced by the CPC since October 1978 (Gelman et al. 1986). These data are referred to as CPC analyses (to differentiate from NCEP reanalyses). The CPC analyses are based on a successive-correction objective analysis (Finger et al. 1965) for pressure levels 70, 50, 30, 10,

5, 2, 1 and 0.4 hPa, incorporating TOVS and ATOVS satellite data and radiosonde measurements (in the lower stratosphere of the NH). This analysis technique has been nearly constant over time (October 1978–April 2001). Horizontal winds are derived from the geopotential data using the ''linear balance'' technique (Randel 1987). The CPC analyses were changed beginning in May 2001, with the data up to 10 hPa based on NCEP, and fields above 10 hPa based solely on ATOVS. Extensive climatologies of the stratosphere have been derived from these CPC data by Hamilton (1982), Geller et al. (1983), and Randel (1992).

The TOVS temperatures used in the CPC analyses have been provided by a series of operational NOAA satellites; these instruments do not yield identical radiance measurements for a variety of reasons, and derived temperatures may change substantially when a new instrument is introduced (Nash and Forrester 1986). Finger et al. (1993) have compared the CPC temperatures in the upper stratosphere (pressure levels 5, 2, 1, and 0.4 hPa) with collocated rocketsonde and lidar data, noting systematic biases of order ± 3–6 K, and provide a set of recommended corrections, which have been incorporated in the results shown here. However, in spite of these adjustments, the CPC analyses still probably retain artifacts of these satellite changes.

4) NCEP

The NCEP–NCAR reanalysis project uses a global numerical weather analysis/forecast system to perform data assimilation using historical observations, spanning the time period from 1957 to the present (Kalnay et al. 1996; Kistler et al. 2001), which for brevity is referred to as NCEP here. The model used in the NCEP has 28 vertical levels, extending from the surface to $\sim$40 km, and analyses of winds, temperatures, and geopotential height are output on stratospheric pressure levels of 100, 70, 50, 30, 20, and 10 hPa. Trenberth and Stepaniak (2002) have documented some spurious problems in the upper-level NCEP stratospheric analyses, but these are mostly evident in highly derived quantities (such as the divergence field), with less influence on analyzed temperatures or winds. It should be noted that substantial changes occur in the NCEP stratospheric data between the pre- and postsatellite data eras (changing in late 1978; see SPARC 2002; Huesmann and Hitchman 2003). The comparisons here focus on the post-1979 time period.

5) ERA-15

The ECMWF produced a global reanalysis for the period 1979–93, based on data assimilation coupled with a numerical forecast model (Gibson et al. 1997). The forecast model used in that work spanned pressure levels 1000–10 hPa, with analyses output on stratospheric pressure levels of 100, 50, 30, and 10 hPa. Because the model has very low stratospheric resolution, and the 10-hPa analysis level is at the top level of the model, upper-level analyses often show spurious results (as evident in the comparisons below).

6) ERA-40

ECMWF has also produced an updated reanalysis, termed ERA-40, covering the period 1957–2001. ERA-40 includes a comprehensive set of global meteorological analyses, including the stratosphere up to 1 hPa, based on the use of variational data assimilation techniques. One important difference from ERA-15 (in addition to the increased vertical domain) is that ERA-40 directly assimilates TOVS and ATOVS radiances, as opposed to retrieved temperature profiles. ERA-40 is available on 23 standard pressure levels spanning 1000–1 hPa, and also on each of the 60 levels of the assimilation model. Documentation of the ERA-40 data assimilation system and subsets of data are available on the ECMWF Web site (online at http://www.ecmwf.int).

7) FUB

The meteorological analyses from the Free University of Berlin (FUB) are northern hemispheric–gridded products at four levels: 100, 50, 30, and 10 hPa. Monthly mean data at these levels are available since 1957 (geopotential height) and 1964 (temperature) on a 10° grid, with an increase in resolution to 5° in the early 1970s. The analyses ended in 2001. Daily analyses are produced only at the three upper levels (i.e., not at 100 hPa) and are provided only every second day in northern summer, when the flow evolves slowly. The analyses were performed by hand (subjective analysis) by experienced personnel, using station observations of geopotential height, wind, and temperature (incorporating hydrostatic and thermal wind balances). Full details of FUB, together with the entire dataset, are available in compact disk (CD) format (Labitzke et al. 2002).

8) CIRA86

The 1986 CIRA (CIRA86) zonal mean temperature, geopotential height, and zonal wind has been described in detail in Barnett and Corney (1985a,b) and Fleming et al. (1988, 1990). These reference climatologies extend from 0 to 120 km and are based on a variety of data sources, briefly summarized here.

Temperatures for 1000–50 hPa are taken from the climatology of Oort (1983), which is based primarily on radiosonde data from the 1960s and early 1970s. Temperatures at 30 hPa over the NH are taken from FUB, and for the SH are taken from the radiosonde climatology of Knittel (1974). For 10–2.5 hPa, values are based on satellite data from the NOAA meteorological satellite *Nimbus-5* selective chopper radiometer (SCR) averaged over 1973–74. From 2.5 to 0.34 hPa

(~40–56 km), the SCR data were merged with temperatures from the *Nimbus-6* pressure modulator radiometer (PMR) averaged over the period July 1975–June 1978. The PMR data were used exclusively for 0.34–0.01 hPa (~56–80 km). All values were merged to obtain a smooth transition between the original datasets.

The zonal wind climatology in the troposphere is taken from Oort (1983), with winds in the middle atmosphere above 100 hPa based on gradient winds derived from the geopotential height climatology. At the equator, the zonal wind (above 100 hPa) is based on the second derivative of geopotential height (Fleming and Chandra 1989).

9) HALOE

The HALOE instrument on *UARS* provides analyses of temperatures in the altitude range ~45–85 km (Russell et al. 1993; Hervig et al. 1996; Remsberg et al. 2002). HALOE uses a solar occultation measurement technique, providing 15 sunrise and 15 sunset measurements per day, with each daily sunrise or sunset group near the same latitude on a given day. The latitudinal sampling progresses in time, so that much of the latitude range ~60°N–S is sampled in 1 month. The vertical resolution of the retrieved temperature profiles is 3–4 km, with sampling on the UARS standard pressure levels (six levels per decade of pressure). The results included here are based on HALOE retrieval version 19.

The seasonal temperature analyses shown here use the combined sunrise plus sunset temperatures binned into monthly samples. The seasonal cycle is derived by a harmonic regression analysis of these monthly data over the period January 1992–December 1999, including annual and semiannual harmonics at each height and latitude (spanning 60°N–S). This regression provides a useful method of interpolating the irregular temporal sampling of HALOE.

10) MLS

Middle atmosphere temperatures have also been obtained from the MLS instrument on *UARS* (Fishbein et al. 1996). The data shown here are from an independent retrieval described in Wu et al. (2002), covering the period January 1992–December 1994. The valid altitude range is 20–90 km, with large uncertainties at the two ends; the temperature is reported on the UARS standard pressure grid (six per decade of pressure), but the actual retrieval was carried out at every other pressure surface. Compared to the MLS version 5 (V5) retrieval, the data presented here have much better vertical resolution in the mesosphere, and about the same resolution in the stratosphere. These data and further descriptions are available to the research community (information online at ftp://mls.jpl.nasa.gov/pub/outgoing/dwu/temp).

The orbital characteristics of *UARS* allow MLS to obtain data from approximately 80°S–32°N or 32°S–80°N for alternating satellite yaw cycles (each approximately 1 month long). In order to handle these large data gaps in high latitudes, our analyses fit the seasonal cycle at each latitude and pressure level using harmonic regression analyses of monthly sampled data (including annual and semiannual harmonic terms in the analyses).

11) URAP

As part of URAP, Swinbank and Ortland (2003) compiled a wind dataset, using measurements from the UARS High Resolution Doppler Imager (HRDI; Hays et al. 1993), supplemented with data from METO. The dataset comprises zonal mean wind data from the earth's surface to the lower thermosphere every month for a period of about 8 yr, starting from the launch of *UARS*. The climatology here use statistics averaged over 1992–98. The wind data are archived on the UARS standard pressure levels, for latitudes from 80°S to 80°N. Figure 1 shows January and July climatological zonal winds derived from the URAP dataset, highlighting the continuous data availability over 0–85 km (note the deep vertical structure of the stratospheric–mesospheric jets). For reference, Fig. 1 also includes corresponding temperature climatologies, derived from combined METO, HALOE, and MLS data (as described in SPARC 2002).

b. Rocketsonde wind and temperature data

Measurements from small meteorological rockets provide an important source of in situ wind and temperature information for the middle atmosphere, between 25 and 85 km. A program of rocketsonde measurements began in the United States in the late 1950s, and expanded during the 1960s to about a dozen stations, making regular measurements 1–3 times per week. The number of rocketsonde measurements peaked in the late 1970s, at about 1000–1500 yearly, including measurements from the former Soviet Union (USSR), Japan, and several other countries. Most measurements were made at middle latitudes of the NH and at tropical locations. The number of rocketsonde stations and frequency of observations decreased markedly in the 1980s, and by the 1990s fewer than 100 rocketsonde measurements were made globally each year. Details of the rocketsonde measurement technique and their uncertainty characteristics are discussed in SPARC (2002).

The rocketsonde wind and temperature climatologies shown here are based on simple monthly averages, derived by binning all of the available observations during 1970–89. Figure 2a shows the availability of rocketsonde observations for this period as a function of latitude. Results shown here focus on the latitude bin centered at 30°N, (including measurements over 20°–40°), plus tropical measurements

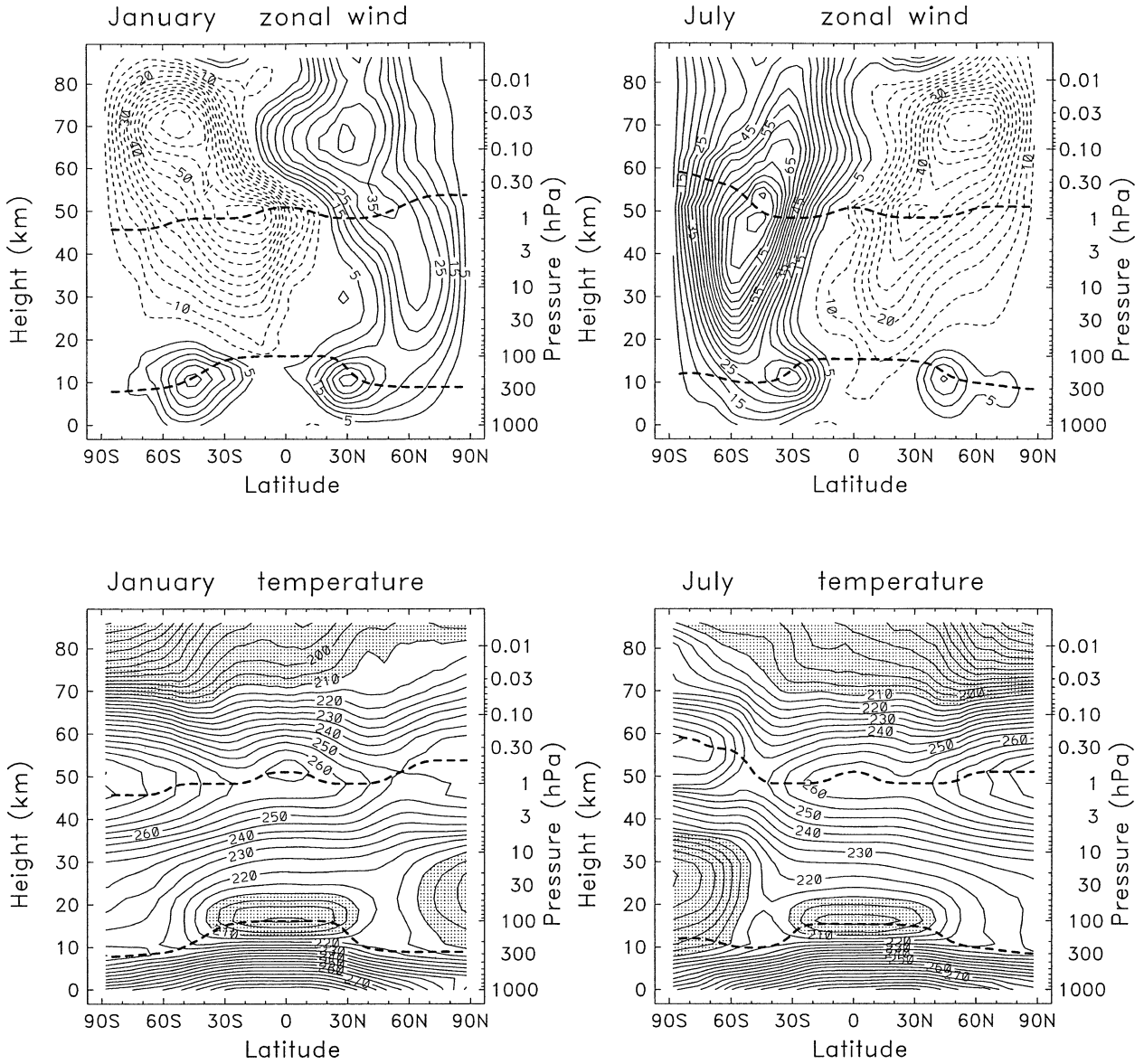

FIG. 1. Climatological zonal mean zonal (top) winds and (bottom) temperatures for (left) Jan and (right) Jul. Zonal winds are from the URAP dataset (contour interval 5 m s^{-1}, with zero contours omitted). Temperatures are from METO analyses (1000–1.5 hPa), and a combination of HALOE plus MLS data above 1.5 hPa (see SPARC 2002). The heavy dashed lines denote the tropopause (taken from NCEP) and stratopause (defined by the local temperature maximum near 50 km).

near 10°S (mostly from Ascension Island at 8°S), and near 10°N (mostly from Kwajelein, Marshall Islands, at 8°N and Fort Sherman, Panama, at 9°N). Based on this sampling, there are approximately 100–300 profile observations in each monthly bin, depending on latitude and altitude. Vertical sampling is made on the UARS pressure grid (six levels per decade of pressure).

Two important considerations apply to the comparisons of rocketsonde data with global analyses. First, the time periods compared here for the data are different (1992–97 for the analyses, and 1970–89 for the rocketsondes). This is most important for temperatures in the upper stratosphere and mesosphere, which have experienced strong cooling (of order 2 K decade^{-1} near the stratopause, and possibly larger in the mesosphere) during the recent decades (Dunkerton et al. 1998; Ramaswamy et al. 2001). A large part of the observed rocketsonde analysis differences in these regions can be attributed to this cooling. Second, the monthly samples from analyses are based on zonal and monthly means of daily data, whereas the rocketsonde statistics are derived from infrequent samples at specific locations, taken over many years. Thus, variability levels for the rocketsonde means are significantly larger. Estimates of the standard error for

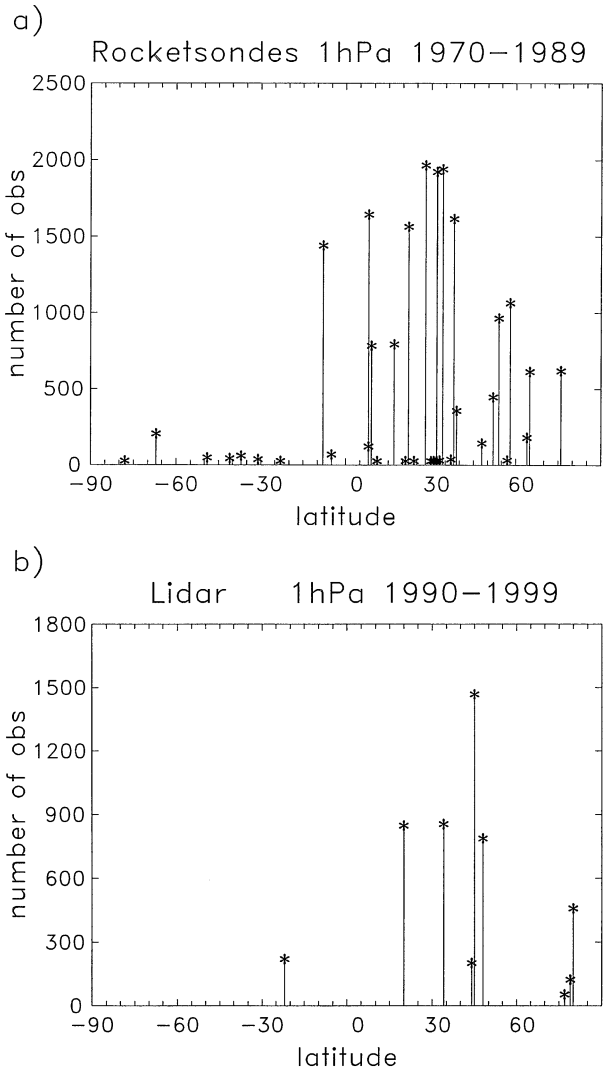

FIG. 2. (a) The availability of rocketsonde wind and temperature measurements at 1 hPa as a function of latitude during 1970–89. Each line represents data from a single station, which are subsequently sampled in latitude bins centered at 10°S, 10°N, 30°N, 60°N, and 80°N. (b) The number and latitude distribution of lidar temperature measurements during the 1990s, which contribute to the lidar climatology.

the monthly rocketsonde (and lidar) data are calculated as $\sigma_{\text{climatology}} = \sigma/\sqrt{N}$, where σ is the standard deviation of the individual soundings within each month and latitude bin, and N is the number of measurements.

c. Lidar temperature data

Lidars provide measurements of the vertical temperature profile in the middle atmosphere, and a number of specific sites have made lidar temperature measurements for a decade or longer. The Rayleigh lidar technique uses the backscattering of a pulsed laser beam to derive the vertical profile of atmospheric density, from which the temperature profile is deduced (Hauchecorne and Chanin 1980; Keckhut et al. 1993). This technique provides an absolute temperature measurement over altitudes ~30–75 km, which does not require adjustment or external calibration. The vertical resolution of the lidar data is approximately 3 km, and the profiles here are sampled on the UARS standard pressure grid.

For the climatological analyses shown here, we obtained a number of lidar temperature time series (for stations with relatively long records) from the Network for the Detection of Stratospheric Change (NDSC) Web site (available online at http://www.ndsc.ws/). The total number of lidar observations and their latitudinal sampling is shown in Fig. 2b. The individual profiles are binned into monthly samples (using all the lidar observations over 1990–99), and we focus here on the latitude bin centered at 40°N, including measurements from Hohenpeissenberg, Germany (48°N); Observatoire de Hante Provence (OHP), France (45°N); Toronto, Ontario, Canada (44°N); and Table Mountain (34°N). This monthly and latitudinal sampling provides ~300 measurements per month. The associated monthly means and standard deviations are calculated identically to those for the rocketsonde analyses.

3. Data intercomparisons

In order to make the most direct comparisons among the different datasets, the first requirement is to choose a time period that maximizes record length for overlap among the most datasets. Here, we choose the period January 1992–December 1997, which gives direct overlap of METO, CPC, NCEP, and ERA-40, and FUB fields. The UKTOVS record is slightly shorter (to April 1997). ERA-15 has a much shorter record during this 1992–97 period (January 1992–December 1993), and comparisons for these data use *differences* only over this 1992–93 record, rather than the full 6 yr, 1992–97. We also include CIRA86, although it should be kept in mind that these data are derived from a very different time period (covering the 1960s–1970s). Rocketsonde data span 1970–89, while lidar temperatures cover 1990–99.

a. Temperature

The latitudinal structure of 100-hPa temperature in January for each analysis is shown in Fig. 3a. The overall latitudinal structure is similar in each dataset, and comparisons are best made by considering differences with a single reference. Differences with respect to the METO 100-hPa analyses are shown in Fig. 3b; the largest differences occur in the Tropics and also over the Arctic. These tropical and polar differences are also observed in other months (not shown here), and discussed in turn below.

Temperatures near the tropical tropopause (~100 hPa) present special problems for analyses, because of

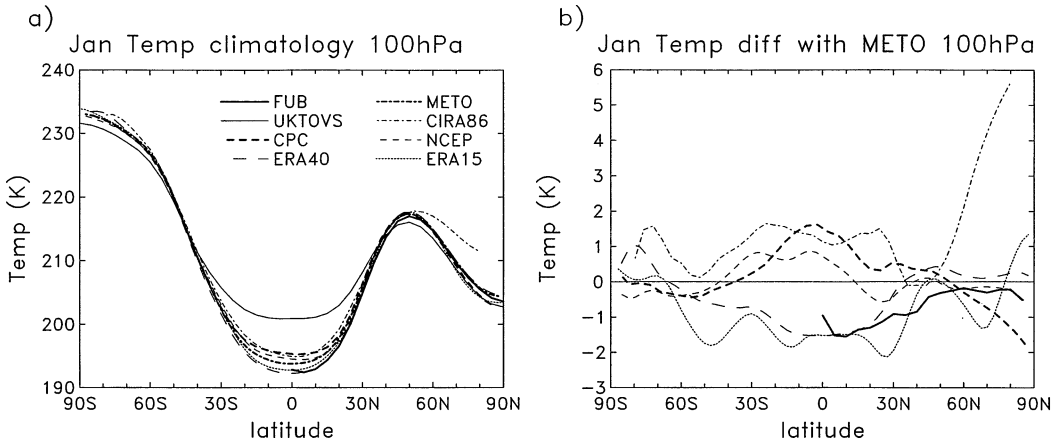

FIG. 3. (a) Latitudinal distribution of 100-hPa zonal mean temperature from different analyses for Jan, together with (b) the distribution of differences between each analysis and METO (i.e., NCEP − METO, etc.). UKTOVS data are an outlier, and not included in (b).

the sharp vertical structure that is not well resolved by satellite measurements, and this region is also problematic for assimilation–forecast models with vertical resolution of ~2 km. The seasonal variations of equatorial temperature at 100 hPa derived from each climatological dataset are shown in Fig. 4, showing substantial differences. We also include in Fig. 4 estimates of monthly temperatures derived for the same 1992–97 period from radiosonde measurements at a group of eight near-equatorial stations (within 5° of the equator, including Belem, Brazil; Bogota, Columbia; Cayenne, French Guiana; Manaus, Brazil; Nairobi, Kenya; the Seychelles; Singapore; and Tarawa, Kiribati). The amplitude of the seasonal cycle in temperature is reasonably well captured in most datasets at 100 hPa, but there are clear biases (as also shown in Pawson and Fiorino 1998a). In particular, the ERA-15, ERA-40, and FUB data are the coldest and agree best with radiosondes, whereas METO, CPC, NCEP, and CIRA86 data each have a consistent warm bias of ~2–3 K (and UKTOVS is almost 10 K too warm, and not shown in Fig. 4).

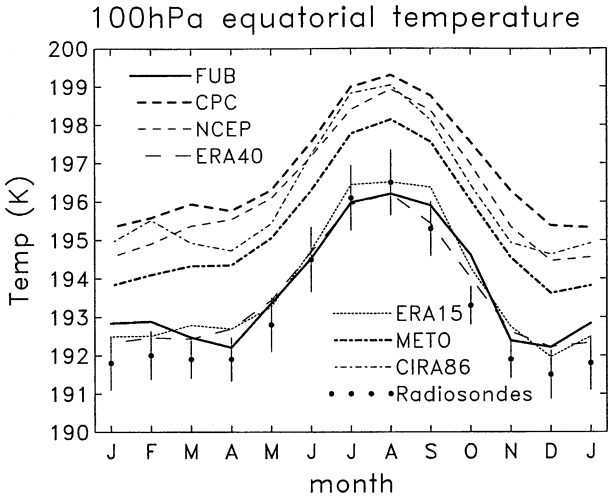

FIG. 4. Comparison of the seasonal variation in 100-hPa equatorial zonal mean temperature from available analyses. The circles show a climatology derived from radiosonde measurements at eight near-equatorial stations (over 5°N–5°S), and the error bars denote the plus/minus standard error of the mean.

As seen in Fig. 3, there can be substantial differences in climatologies of polar temperature in the lower stratosphere. Figure 5 compares the seasonal cycle of 50-hPa zonal mean temperature in both polar regions (80°N and 80°S), including their respective differences with METO. The CIRA86 data exhibit warm biases by up to ~5 K in the Arctic and ~10 K in the Antarctic, maximizing during winter–spring in each hemisphere. A large portion of these differences reflects true cooling in the polar lower stratosphere between the 1960s and 1990s (e.g., Randel and Wu 1999; Ramaswamy et al. 2001). Aside from CIRA86, the other climatologies agree to approximately ±1 K in the Arctic and ±2 K in the Antarctic. Most analyses are colder than METO during Arctic winter, suggesting a small, warm METO bias. Similar comparisons and results for CPC and METO data have been shown by Manney et al. (1996).

Zonal mean temperature comparisons in the middle and upper stratosphere (not shown here, but see SPARC 2002) reveal relatively larger differences (typically ±2–4 K) than at 100 or 50 hPa, and each dataset has characteristic patterns of differences (typically larger over high latitudes). The CIRA86 and MLS data are consistently on the warm side of the ensemble throughout the stratosphere, while ERA-40 has cold biases of ~5 K over ~5–2 hPa. NCEP and ERA-15 data have persistent biases near 10 hPa, which is the top level of their analyses. Comparisons at 1 hPa (see below) show a range of mean differences of order ~5 K. This level near the stratopause presents special problems in analyses, because it is not captured accurately in the TOVS thick-layer radiance measure-

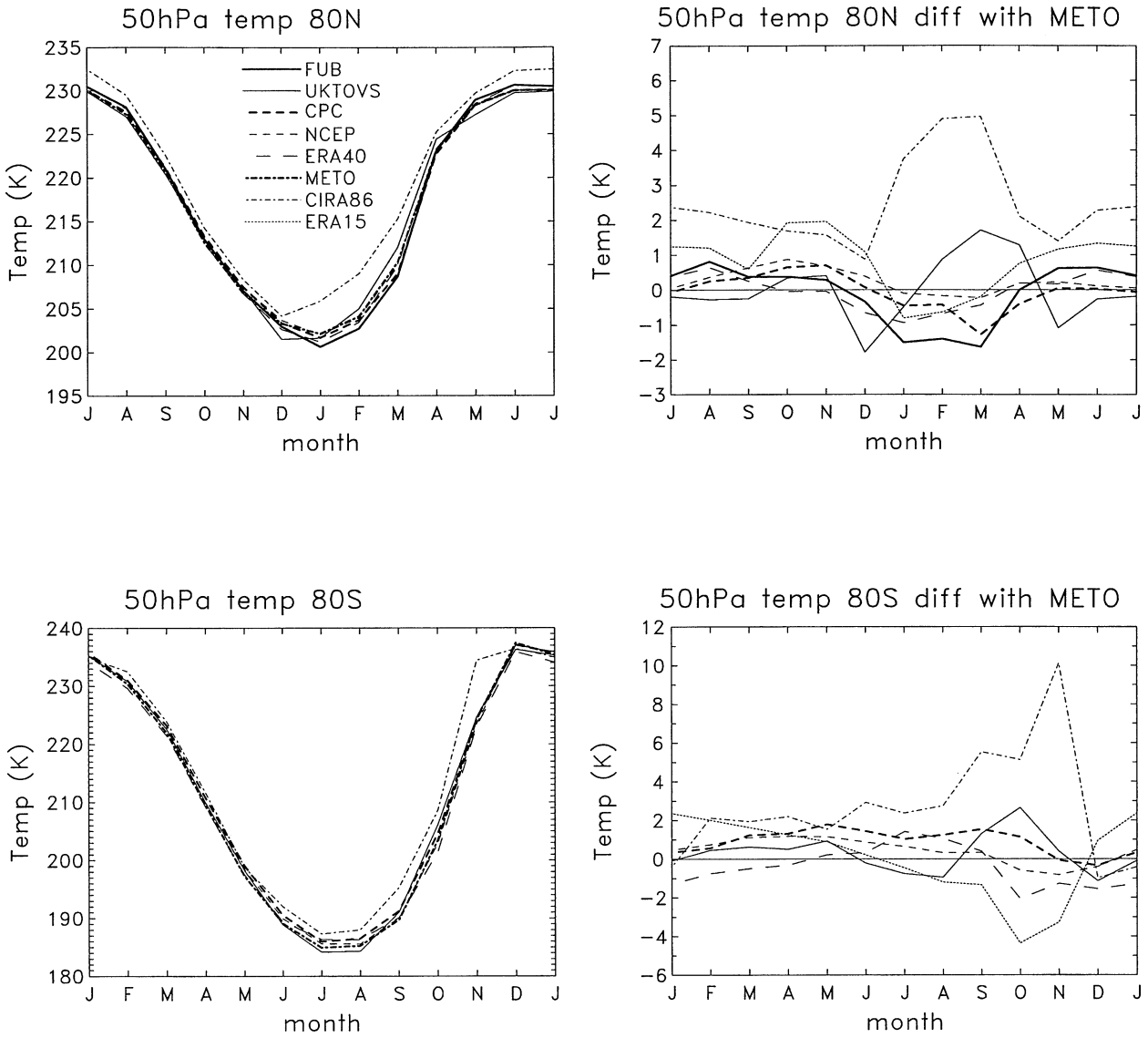

FIG. 5. (left) Seasonal variations of 50-hPa zonal mean temperature at (top) 80°N and (bottom) 80°S are shown; note the respective time axes have been shifted by 6 months so that winter is in the middle of each plot. (right) The corresponding differences from METO analyses are also shown (i.e., CIRA86 − METO, etc.).

ments, and it is near the top of the METO forecast–assimilation model (at 0.3 hPa).

1) COMPARISONS WITH ROCKETSONDES

Figure 6 compares rocketsonde climatological temperature profiles with zonal mean analyses at 30°N for January, including differences of the different data with respect to METO (up to 0.3 hPa). Most analyses show reasonable agreement in the stratosphere (to within ±2 K), except for CIRA86 and MLS (warm biases of ~4–6 K), and ERA-40 (cold biases of ~5 K near 40 km). The rocketsondes show good overall agreement in the stratosphere, and in the location of the stratopause. However, the rocketsonde temperatures near the stratopause and in the mesosphere (~45–70 km) are warmer than the other climatologies, and this is a consistent feature of the rocketsondes that is at least partially due to the differing respective time periods.

The seasonal variation of temperatures near 30°N from rocketsondes and zonal mean analyses are compared in Fig. 7, for data at 1 and 0.1 hPa. At 1 hPa there are mean biases of the order of 5 K between the climatologies, and the rocketsonde temperatures are on the warm side of the ensemble. At 0.1 hPa the mean rocketsonde values are ~4–10 K warmer than MLS or HALOE data, and ~2–8 K warmer than CIRA86, and the rocketsonde differences are largest during the NH winter (October–March). Even larger rocketsonde dif-

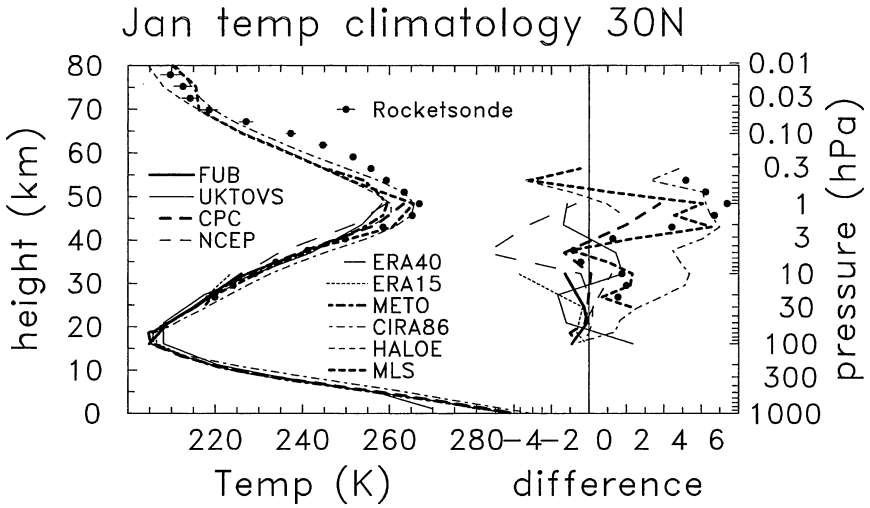

FIG. 6. Comparison of Jan average rocketsonde temperature statistics at 30°N with zonal mean analyses. Right-hand side shows the respective differences from METO analyses up to 0.3 hPa.

ferences (~10–20 K) are found for comparisons at 60°N (SPARC 2002). Note that while the warm mesospheric biases with respect to HALOE and MLS can be partially attributed to the different respective time periods, this is not the case for the difference with CIRA86 (derived from satellite data from the 1970s).

2) Comparisons with lidars

The lidar temperature measurements are contemporaneous with the global analyses, and offer the most direct comparisons. The seasonal comparison of temperatures near 40°N at 10, 1, and 0.1 hPa are shown in Fig. 8 (averaged lidar data and zonal mean analyses). The comparisons at 10 hPa show overall excellent agreement for most of the year (with CIRA86 and UKTOVS as warm outliers), although the lidars show some cold biases in early winter (due to spatial sampling, as shown below). The lidars fall in the midrange of analyses at 1 hPa, and exhibit reasonably good agreement at 0.1 hPa (although they are biased warm during equinox seasons). The overall agreement between the lidar and satellite data at 0.1 hPa in Fig. 8 is further evidence that the larger differences with rocketsondes in the mesosphere (Figs. 6–7) are primarily due to the different time periods covered.

The influence of the limited spatial sampling of the lidar data is illustrated in Fig. 8d, showing the 10-hPa lidar averages and METO zonal means, plus the METO data sampled at the four lidar sites. Differences of the order of 3–5 K are found between the two samples of METO data during the NH winter (November–March), and the METO data sampled at the lidar sites agree much better with lidar measurements than do the METO zonal means. The differences are due to the time mean asymmetries in the winter stratosphere (stationary planetary waves), combined with the limited lidar sampling (over western Europe and North America). Similar sampling issues probably also occur in the winter mesosphere, when stationary planetary waves are large.

3) Semiannual oscillation in tropical temperatures

Seasonal temperature variations in the Tropics at and above 10 hPa are dominated by a semiannual oscillation (SAO), and here we quantify the SAO amplitude and phase structures derived from the different datasets. A comprehensive review and climatology of the SAO (extending to 100 km) is provided in Garcia et al. (1997). The results here are based on simple harmonic analyses of the different datasets for the periods available.

Figure 9a shows the amplitude structure of the temperature SAO as a function of latitude at 2 hPa as derived from the different datasets. The temperature SAO has a maximum over the equator, falling to small amplitudes at 20°N–S. The different datasets in Fig. 9 show a clear separation in terms of SAO amplitude, with the ERA-40, MLS, HALOE, and CIRA86 data having amplitudes near 4 K, approximately twice as large as the CPC, METO, and UKTOVS results. The rocketsonde results (shown as dots near 8°N and 8°S) show amplitudes that agree better with values from the former (larger amplitude) group.

The vertical structure of the temperature SAO amplitude and phase at the equator are shown in Figs. 9b–9c, including results from each dataset. Rocketsonde results are included by averaging results at 8°N and 8°S (see Fig. 9a), with amplitudes multiplied by a factor of 1.3 to approximate equivalent equatorial values. As is well known from previous analyses (e.g., Hirota 1980), the temperature SAO has a double-peaked structure in altitude, with maxima below the stratopause (~45 km) and mesopause (~70 km), and these maxima are approxi-

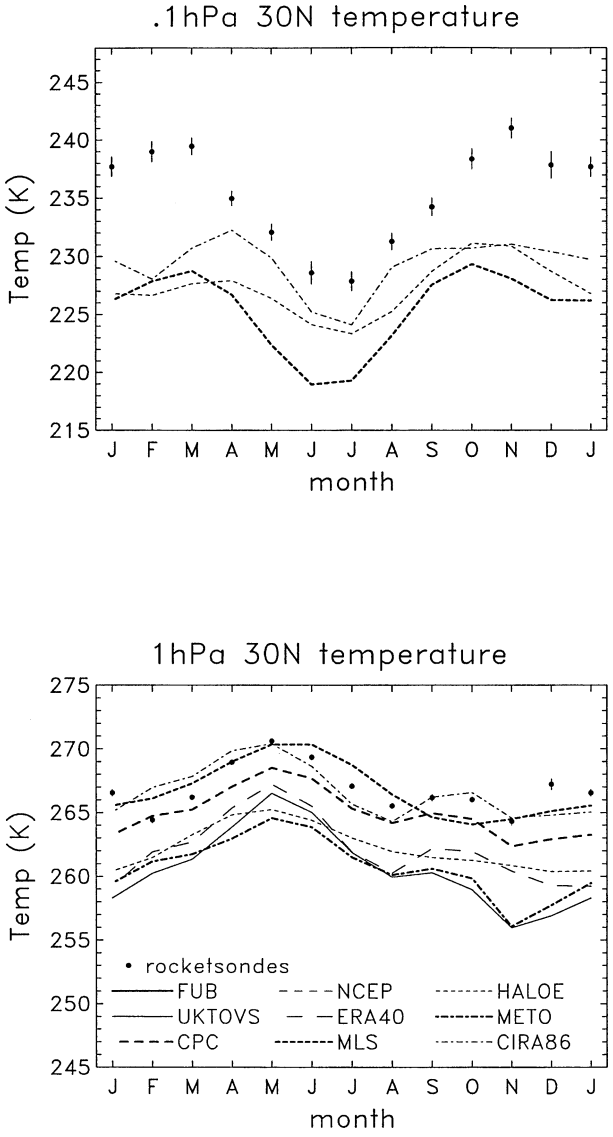

FIG. 7. Comparison of the seasonal variation of rocketsonde temperatures near 30°N with zonal mean analyses, for pressure levels (top) 0.1 and (bottom) 1 hPa. Circles denote the rocketsonde means, and error bars the plus/minus one standard error.

mately out of phase. As noted above, the maximum near 45 km has an amplitude of ~4 K in MLS, HALOE, CIRA86, ERA-40, and rocketsonde datasets, and a substantially weaker amplitude in CPC, METO, and UKTOVS data. For the maximum near 70 km, CIRA86, MLS, and HALOE show a range of amplitudes of ~4–7 K. Also included in Fig. 9 are results derived from Solar Mesosphere Explorer (SME) temperature data for 1982–86 (taken from Garcia and Clancy 1990). These SME results show a similar amplitude and phases as the other datasets, but do not exhibit an absolute peak near 70 km. Note, however, that the SME results may be influenced by aliasing of the migrating tides in the mesosphere (see Garcia and Clancy 1990).

b. Zonal mean zonal winds

Climatological zonal mean zonal winds show overall good agreement among the various datasets in the extratropics, whereas relatively large differences occur in the Tropics. Tropical stratospheric winds present particular problems, because there are few direct wind measurements above the lower stratosphere. Also, due to the smallness of the Coriolis parameter, determination of balanced winds in the Tropics requires more accurate estimates of horizontal temperature gradients. Figure 10 shows cross sections of differences (from METO analyses) of January average zonal winds for CPC, ERA-40, and CIRA86 data (i.e., differences from the January climatology shown in Fig. 1). Differences in extratropics for CPC and ERA-40 are of the order of ~2 m s^{-1}, and this is typical for other months (and for NCEP, ERA-15, and UKTOVS data); slightly larger extratropical differences (up to ~10 m s^{-1}) are found for CIRA86 data. Larger zonal wind differences are seen in the Tropics in Fig. 10, and this is typical across all the datasets. Strong tropical easterly biases are a particular problem in the CIRA86 dataset.

Figure 11 shows further comparisons of zonal winds in the upper stratosphere (5 hPa) and mesosphere (0.1 hPa), at 10°S and 30°N, including results from rocketsondes (which provide direct measurements of zonal winds, and are unique for comparing to analyses). In the upper stratosphere, the rocketsondes show good agreement with analyses both in the Tropics and extratropics. Furthermore, the few available datasets in the mesosphere (CIRA86, URAP, and rocketsondes) show reasonably similar seasonal variability.

1) TROPICAL SEMIANNUAL OSCILLATION

As with temperature, the SAO dominates the seasonal variation of zonal winds in the Tropics above the middle stratosphere. The latitudinal amplitude structure of the zonal wind SAO at 1 hPa is shown in Fig. 12a, comparing each dataset along with rocketsonde results at 8°N and 8°S. The zonal wind SAO shows maximum amplitude near 10–20°S for most datasets, which is distinct from the equatorially centered SAO in temperature (Fig. 9a). The rocketsonde results near 8°N and 8°S suggest a latitudinal asymmetry consistent with analyses, that is, larger zonal wind SAO in the SH subtropics. The rocketsonde SAO amplitudes are approximately 25% larger than most analyses (except for ERA-40), while the phases (not shown) are in good agreement. Figures 12b–12c show the SAO vertical amplitude and phase structure at the equator, including rocketsonde results (taken as averages of 8°N and 8°S, based on the latitudinal structure seen in Fig. 12a). The vertical structure shows an amplitude maximum near the stratopause (~50 km), with a magnitude of ~15–20 m s^{-1} for the analyses; the rocketsondes give a maximum closer

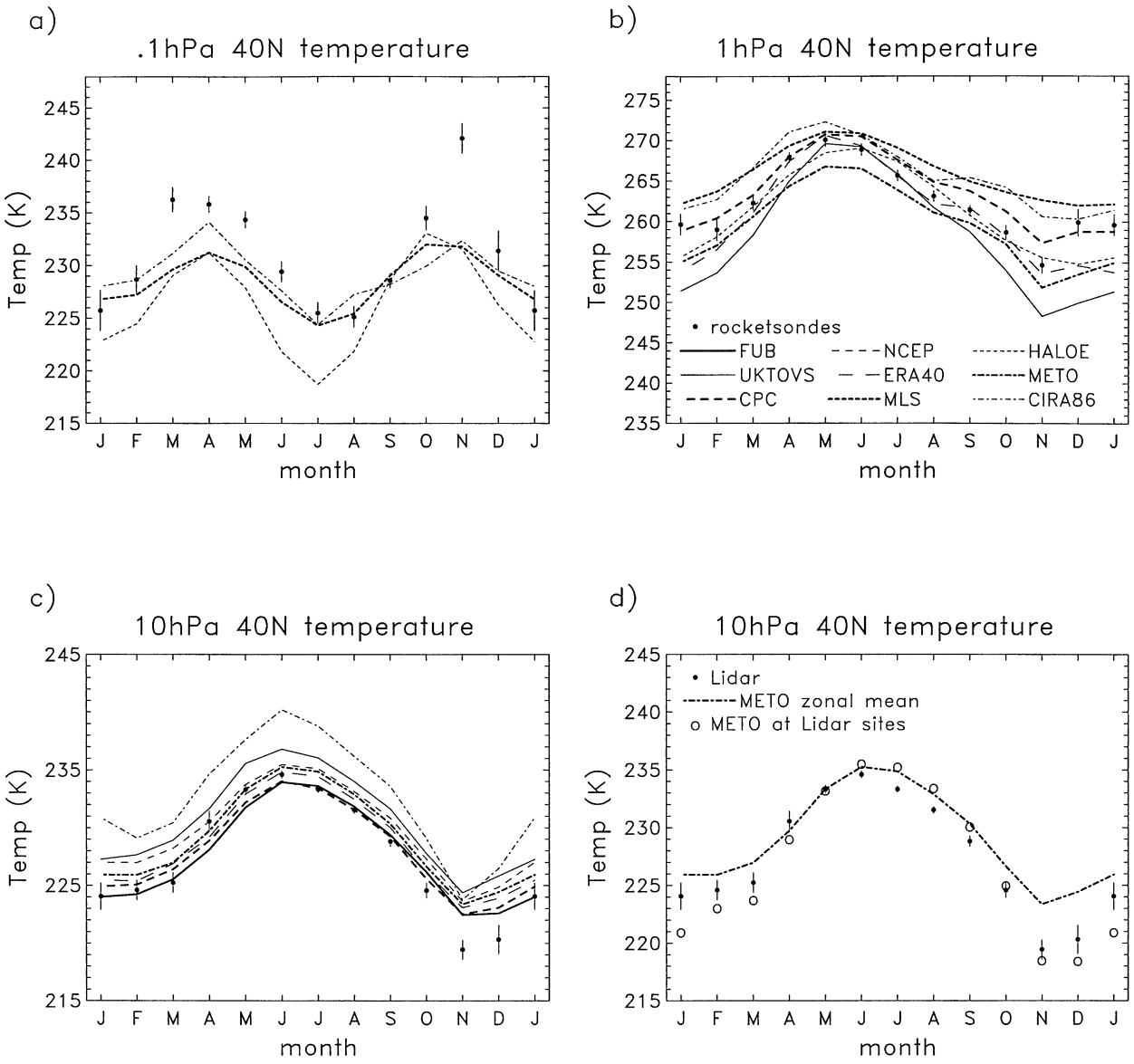

FIG. 8. Comparison of the seasonal variation of lidar temperatures near 40°N with zonal mean analyses, at (a) 0.1, (b) 1, and (c) 10 hPa. Circles denote the lidar means, and error bars the plus/minus one standard error. (d) The 10-hPa results for lidars and zonal mean METO, plus the METO data sampled at the four lidar locations are shown.

to 25 m s^{-1}. A second amplitude maximum near the mesopause (~80 km) is suggested in URAP and CIRA86 winds.

2) THE QUASI-BIENNIAL OSCILLATION

The quasi-biennial oscillation (QBO) dominates interannual variability for zonal winds in the Tropics, but there are significant differences in magnitude derived from various datasets (e.g., Pawson and Fiorino 1998b). This is evident in Fig. 13, showing interannual anomalies in equatorial zonal wind at 30 and 10 hPa, during 1988–97, derived from the various analyses. Also included in Fig. 13 are anomalies derived from Singapore radiosonde data, which are a standard reference for the QBO (e.g., Naujokat 1986). While the QBO signal is evident in each dataset, the amplitude varies strongly between different data (and with altitude). In general the assimilated datasets (METO, NCEP, ERA-15, and ERA-40) have the largest, most realistic amplitudes, whereas the balance winds derived from CPC and UKTOVS are much too weak. ERA-40 appears best at capturing the strength of the westerly phase at 10 hPa.

The strength of the zonal wind QBO in the different datasets is quantified in Fig. 14, where the equivalent QBO amplitude (defined as $\sqrt{2}$ times the rms deviation of deseasonalized anomalies during 1992–97) is

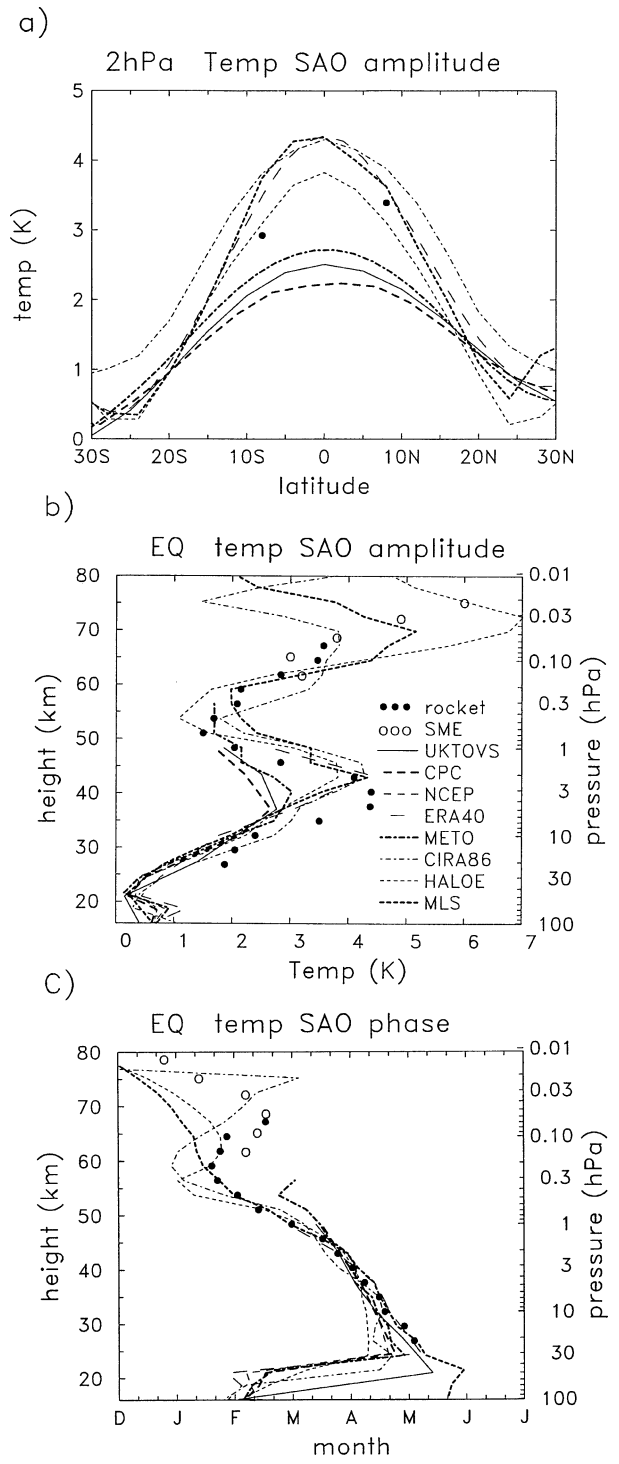

FIG. 9. (a) Latitudinal structure of the amplitude of the temperature SAO at 2 hPa derived from each dataset. The dots show the corresponding values derived from rocketsonde data near 8°S and 8°N. (b) The vertical amplitude and (c) phase structure of the SAO at the equator are shown. Phase refers to month of the first maximum during the calendar year. The open circles show the mesospheric results derived from SME satellite data, taken from Garcia and Clancy (1990).

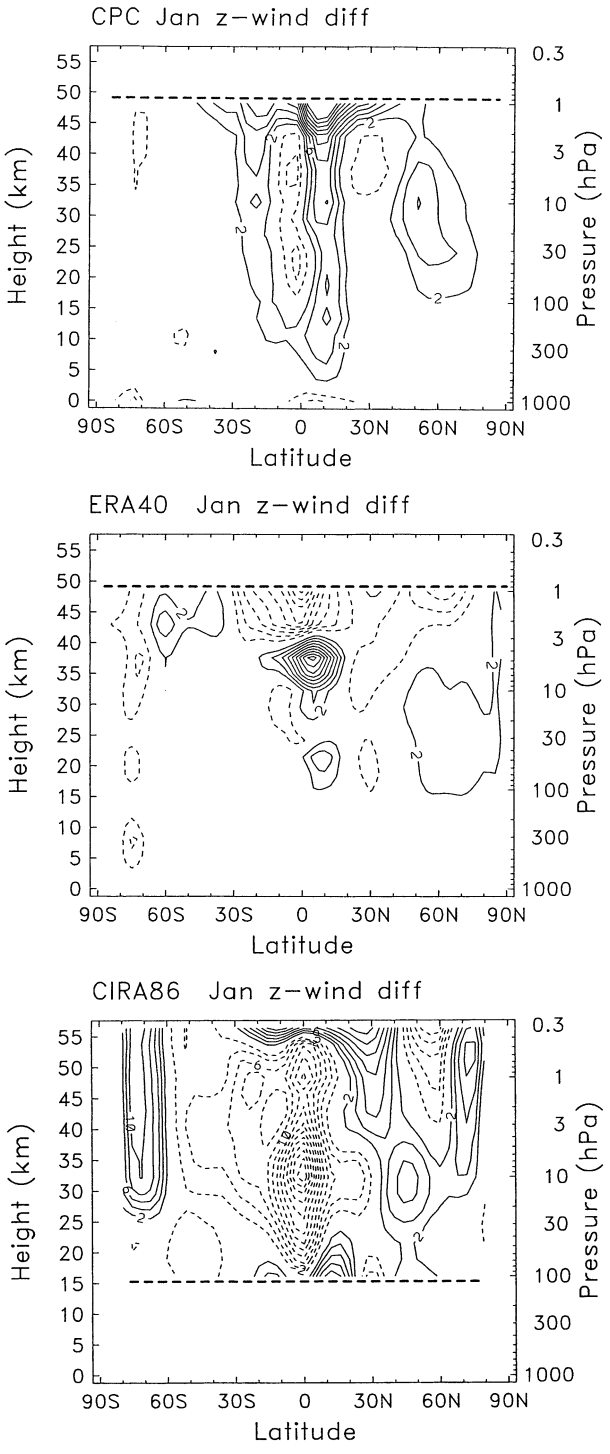

FIG. 10. Meridional cross sections of differences in Jan zonal mean zonal wind from METO, showing results for (top) CPC, (middle) ERA-40, and (bottom) CIRA86. Contour intervals are ±2, 4, 6 . . . m s^{-1}.

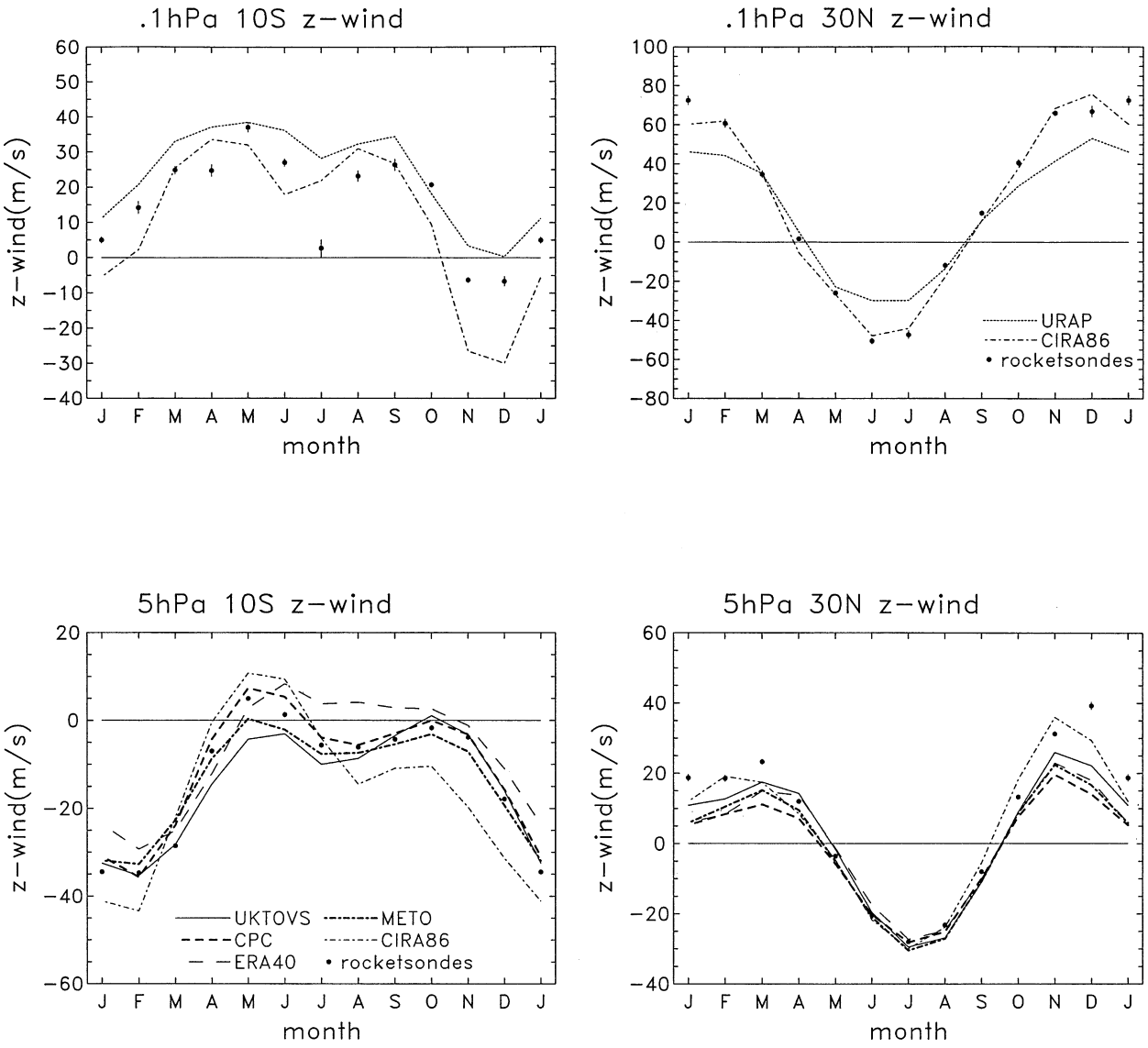

FIG. 11. Comparison of the seasonal variation of zonal winds measured by rocketsondes with zonal mean analyses at (left) 10°S and (right) 30°N, for statistics at (top) 0.1 and (bottom) 5 hPa.

plotted as a function of latitude (at 30 hPa) and height. Figure 14 also includes the 30-hPa QBO amplitude derived from tropical radiosonde climatologies in Dunkerton and Delisi (1985), plus an equivalent QBO amplitude derived from rocketsonde data during 1970–89, for altitudes ~24–37 km (where a strong QBO is evident by eye in the deseasonalized time series). For the analysis datasets, ERA-40 exhibits the largest QBO amplitude (in best agreement with the radiosonde climatology and Singapore data), with ERA-15, METO, and NCEP somewhat weaker, and CPC and UKTOVS (balance winds) as severe underestimates. The ERA-40, ERA-15, METO, and NCEP datasets show approximately similar amplitudes between 70 and 30 hPh, whereas above 30 hPa there are larger differences. Only ERA-40 approaches the Singapore and rocketsonde amplitudes over 20–10 hPa. Above 10 hPa there is a factor of two difference between the ERA-40 and METO results, and here the METO data are almost certainly too weak.

4. Summary: Biases and outstanding uncertainties

This study has focused on comparing climatological datasets for the middle atmosphere that are currently used in the research community. Overall, the climatologies developed from analyses (and lidar measurements) for the 1990s agree well in most aspects, although each global dataset can exhibit ''outlier'' behavior for certain statistics. The following is a list of the largest apparent biases in each climatological dataset, as derived from the intercomparisons discussed here and in SPARC

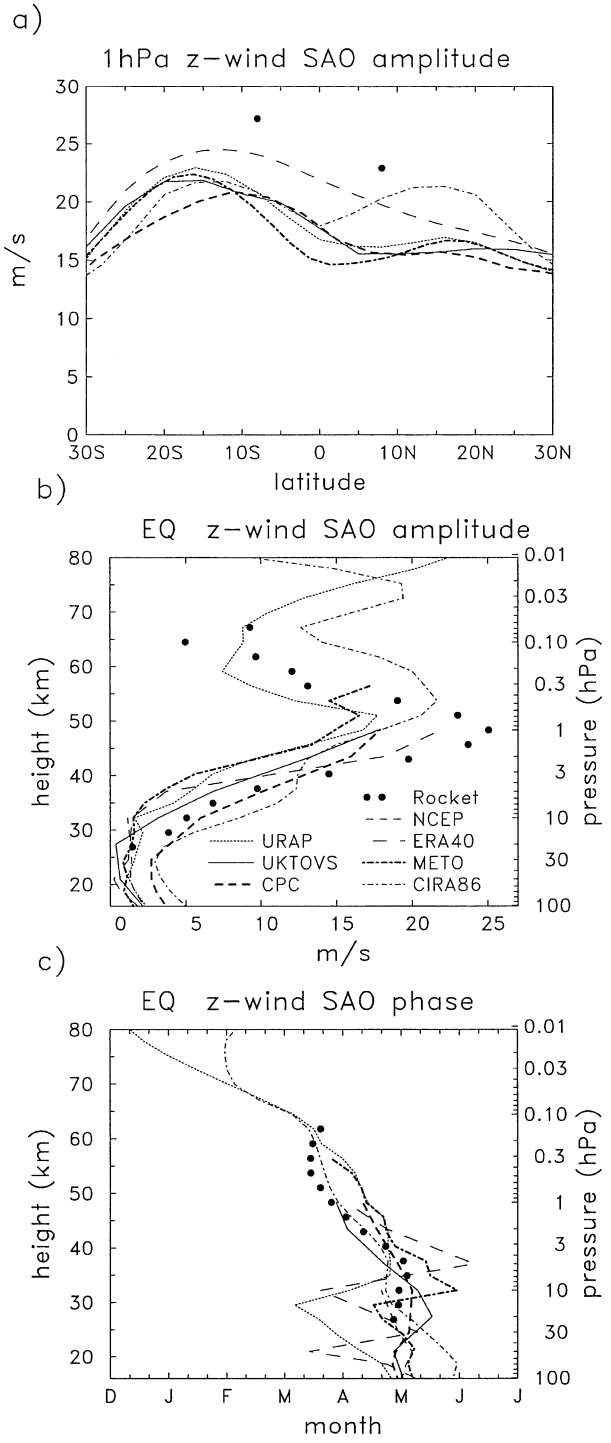

FIG. 12. (a) Latitudinal structure of the zonal wind SAO at 1 hPa derived from each dataset. Dots show rocketsonde results at 8°N and 8°S. (b) The vertical amplitude and (c) phase of the zonal wind SAO at the equator are shown. The phase refers to the time of the first maximum during the calendar year.

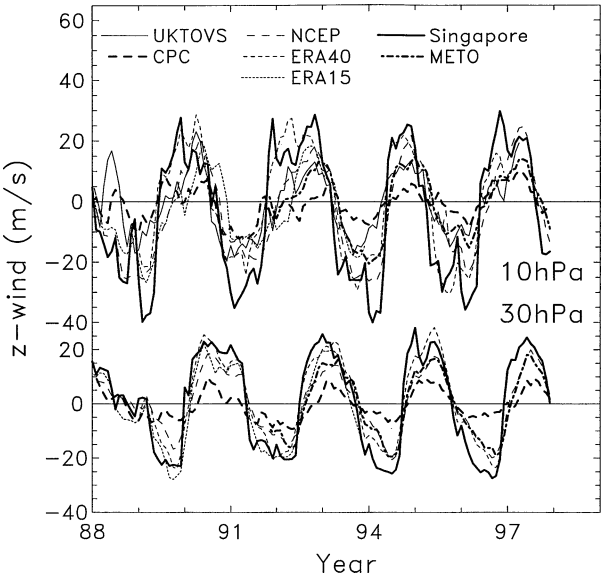

FIG. 13. Time series of interannual anomalies in equatorial zonal mean winds during 1988–97 at 10 and 30 hPa from various analyses and from Singapore (1°N) radiosonde measurements. Each dataset has been deseasonalized with respect to the 1992–97 means.

(2002). These are identified when individual datasets are outliers from the group, for these particular features.

METO
- cold temperature biases (~5 K) near the stratopause (globally)
- warm tropical tropopause temperature (1–2 K)

UKTOVS
- large temperature biases (~±3–5 K) in low latitudes (~30°N–S) over much of the stratosphere (20–50 km)
- winter polar night jets somewhat too strong
- weak tropical wind variability (derived from balanced winds)

CPC
- warm temperature biases (~1–3 K) in the Antarctic lower stratosphere during winter–spring
- weak tropical wind variability (derived from balanced winds)
- warm tropical tropopause temperatures (2–3 K)
- weak eddy fluxes in SH

NCEP
- warm tropical tropopause (2–3 K)
- satellite data discontinuity across 1978–79

ERA-15
- global cold biases (~3 K) at 30 and 10 hPa

ERA-40
- cold temperature biases (~5 K) in the upper stratosphere (2–5 hPa)
- oscillatory vertical structure in temperature, especially large over Antartica

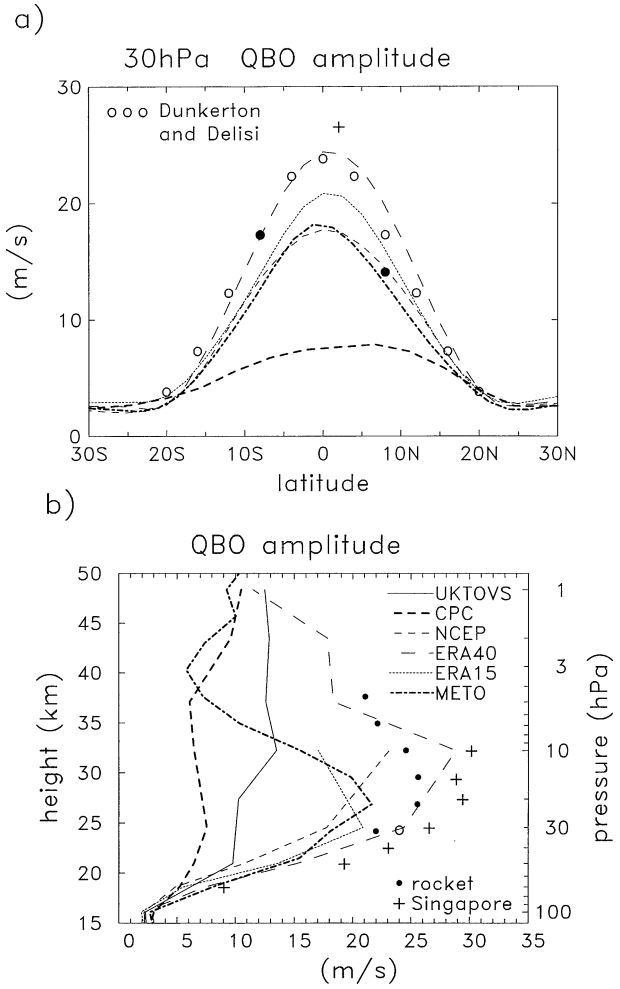

FIG. 14. (a) Latitudinal structure of the equivalent QBO amplitude in zonal wind at 30 hPa, defined as $\sqrt{2}$ times the rms anomaly values during 1992–97 (see text). (b) The vertical structure of QBO amplitude at the equator is shown. For comparison, results of Dunkerton and Delisi (1985) are shown, together with estimates from Singapore radiosondes and results derived from rocketsondes for 1970–89. The equatorial rocketsonde results in (b) are derived from an average of the values at 8°N and 8°S, multiplied by a factor of 1.5.

CIRA86
- warm biases of ~5–10 K over much of the stratosphere (20–50 km)
- relatively large easterly biases in tropical winds (derived from balanced winds)
- SAOs in mesospheric wind and temperature not well resolved

MLS
- warm biases (~3–7 K) over much of the stratosphere (20–50 km)

Comparisons of the recent climatologies with the historical datasets (CIRA86 and rocketsondes) show reasonable agreement, but the effect of decadal-scale cooling throughout the middle atmosphere is evident, particularly in the polar lower stratosphere (Fig. 5) and in the upper stratosphere and mesosphere (e.g., Figs. 6–7). Decadal changes may also influence zonal mean winds at high latitudes (SPARC 2002). Despite these differences, the overall quality of the global CIRA86 is remarkable, given that they were derived from several combined datasets, covering different altitudes and time periods.

The comparisons presented here also allow us to highlight aspects of middle-atmosphere climatologies that are relatively uncertain. These are identified for statistics that show relatively large variability among each of the different datasets, suggesting a fundamental level of uncertainty or high sensitivity to the details of data analysis. These include the following:

1) The tropical tropopause region is biased warm (compared to radiosonde data) in many analyses. Relatively small biases are found in ERA-15, ERA-40, and FUB, which are more strongly tied to radiosonde measurements. The warm biases in this region of sharp temperature gradients probably result from a combination of low vertical resolution in the analyses, plus the less than optimal use by most analyses of thick-layer satellite radiance measurements.
2) The temperature and ''sharpness'' of the global stratopause shows considerable variability among the different datasets. This is probably due to the relatively low vertical resolution of TOVS satellite measurements, and also to the fact that the stratopause is near the upper boundary for several analyses (METO, CPC, UKTOVS).
3) Temperature variability in the tropical upper stratosphere (associated with the SAO) is underestimated in analyses that rely primarily on low-resolution TOVS satellite data (CPC, UKTOVS, and METO).
4) QBO variations in temperature and zonal wind are underestimated to some degree in most analyses, as compared to Singapore radiosonde data. The best results are derived from the assimilated datasets (ERA-40, ERA-15, METO, and NCEP, in that order) and only ERA-40 has realistic zonal wind amplitudes above 30 hPa. The use of balance winds in the Tropics (derived from geopotential data alone) is problematic for the QBO.

The overall improvements seen in the ERA-40 data for tropical variability suggests that improving data assimilation techniques offer the best opportunity for accurate analyses in the tropical stratosphere.

Acknowledgments. These climatological comparisons have resulted from work of the SPARC Reference Climatology Group, which has been ongoing since 1994. A majority of the work has centered around obtaining and archiving the numerous datasets in the SPARC Data Center. This activity was primarily organized by Dr. Petra Udelhofen, who unfortunately died during the final stages of preparation of the SPARC (2002) report. Petra was a

valued friend and colleague of everyone involved with this project, and we dedicate it to her memory.

We wish to note special thanks to the NASA ACMAP Research Program, for support of the SPARC Data Center, and for supporting several individuals involved with the climatology group. Marilena Stone (NCAR) expertly prepared the manuscript through many drafts. We thank Rolando Garcia, Dan Marsh, and Kevin Trenberth for comments on an early draft. We especially thank Barbara Naujokat for a careful and thorough review of the manuscript, and for pointing out some errors in our earlier calculations.

REFERENCES

Bailey, M. J., A. O'Neill, and V. D. Pope, 1993: Stratospheric analyses produced by the United Kingdom Meteorological Office. *J. Appl. Meteor.,* **32,** 1472–1483.

Barnett, J. J., and M. Corney, 1985a: Middle atmosphere reference model from satellite data. *Middle Atmosphere Program, Handbook for MAP*, K. Labitzke, J. J. Barnett, and B. Edwards, Eds., Vol. 16, SCOSTEP, 47–85.

——, and ——, 1985b: Temperature data from satellites. *Middle Atmosphere Program, Handbook for MAP*, K. Labitzke, J. J. Barnett, and B. Edwards, Eds., Vol. 16, SCOSTEP, 2–11.

Dunkerton, T. J., and D. P. Delisi, 1985: Climatology of the equatorial lower stratosphere. *J. Atmos. Sci.,* **42,** 376–396.

——, ——, and M. Baldwin, 1998: Examination of middle atmosphere cooling trend in historical rocketsonde data. *Geophys. Res. Lett.,* **25,** 3371–3374.

Finger, F. G., H. M. Wolf, and C. E. Anderson, 1965: A method for objective analysis of stratospheric constant pressure charts. *Mon. Wea. Rev.,* **93,** 619–638.

——, M. E. Gelman, J. D. Wild, M. L. Chanin, A. Hauchecorne, and A. J. Miller, 1993: Evaluation of NMC upper stratospheric analyses using rocketsone and lidar data. *Bull. Amer. Meteor. Soc.,* **74,** 789–799.

Fishbein, E., and Coauthors, 1996: Validation of the UARS microwave limb sounder temperature and pressure measurements. *J. Geophys. Res.,* **101,** 9983–10 016.

Fleming, E. L., and S. Chandra, 1989: Equatorial zonal wind in the middle atmosphere derived from geopotential height and temperature data. *J. Atmos. Sci.,* **46,** 860–866.

——, ——, M. R. Schoeberl, and J. J. Barnett, 1988: Monthly mean global climatology of temperature, wind, geopotential height, and pressure for 0-120 km. NASA Tech. Memo. NASA TM-100697, 85 pp.

——, ——, J. J. Barnett, and M. Corney, 1990: Zonal mean temperature, pressure, zonal wind, and geopotential height as functions of latitude, COSPAR International Reference Atmosphere: 1986, Part II: Middle Atmosphere Models. *Adv. Space Res.,* **10,** 11–59.

Garcia, R. R., and R. T. Clancy, 1990: Seasonal variation of equatorial mesospheric temperatures observed by SME. *J. Atmos. Sci.,* **47,** 1666–1673.

——, T. J. Dunkerton, R. S. Lieberman, and R. A. Vincent, 1997: Climatology of the semiannual oscillation of the tropical middle atmosphere. *J. Geophys. Res.,* **102,** 26 019–26 032.

Geller, M. A., M.-F. Wu, and M. E. Gelman, 1983: Troposphere–stratosphere (surface-55 km) monthly winter general circulation statistics for the Northern Hemisphere—Four year averages. *J. Atmos. Sci.,* **40,** 1334–1352.

Gelman, M. E., A. J. Miller, K. W. Jihnson, and R. N. Nagatani, 1986: Detection of long term trends in global stratospheric temperature from NMC analyses derived from NOAA satellite data. *Adv. Space Res.,* **6,** 17–26.

Gibson, J. K., and Coauthors, 1997: ERA description. European Center for Medium-Range Weather Forecasts Reanalysis Project Rep. 1, 77 pp.

Hamilton, K., 1982: Stratospheric circulation statistics. NCAR Tech. Note NCAR/TN-191 STR, 174 pp.

Hauchecorne, A., and M.-L. Chanin, 1980: Density and temperature profiles obtained by lidar between 35 and 70 km. *Geophys. Res. Lett.,* **7,** 565–568.

Hays, P. B., V. J. Arbreu, M. E. Dobbs, D. A. Gell, H. J. Grassl, and W. R. Skinner, 1993: The high-resolution Doppler imager on the Upper Atmosphere Research Satellite. *J. Geophys. Res.,* **98,** 10 713–10 723.

Hervig, M. E., and Coauthors, 1996: Validation of temperature measurements from the Halogen Occultation Experiment. *J. Geophys. Res.,* **101,** 10 277–10 286.

Hirota, I., 1980: Observational evidence of the semiannual oscillation in the middle atmosphere: A review. *Pure Appl. Geophys.,* **118,** 217–238.

Huesmann, A., and M. Hitchman, 2003: The 1978 shift in the NCEP reanalysis stratospheric quasi-biennial oscillation. *Geophys. Res. Lett.,* **30**, 1048, doi:10.1029/2002GL016323.

Kalnay, E., and Coauthors, 1996: The NCAR/NCEP 40-Year Reanalysis Project. *Bull. Amer. Meteor. Soc.,* **77,** 437–471.

Keckhut, P., A. Hauchecorne, and M.-L. Chanin, 1993: A critical review of the database acquired for the long term surveillance of the middle atmosphere by the French Rayleigh lidar. *J. Atmos. Oceanic Technol.,* **10,** 850–867.

Kistler, R., and Coauthors, 2001: The NCEP–NCAR 50-year reanalysis: Monthly means CD-ROM and documentation. *Bull. Amer. Meteor. Soc.,* **82,** 247–267.

Knittel, J., 1974: Ein Beitrag zur Klimatologie der Stratosphaere der Suedhalbkugel. Vol. A2, Meteor. Abh. Met. Inst., 90 pp.

Labitzke, K., and Coauthors, 2002: *The Berlin Stratospheric Data Series.* Meteorological Institute, Free University of Berlin, CD-ROM.

Lorenc, A. C., and Coauthors, 2000: The Met Office global 3-dimensional variational data assimilation scheme. *Quart. J. Roy. Meteor. Soc.,* **126,** 2992–3012.

Manney, G. L., and Coauthors, 1996: Comparison of UK meteorological office and US NMC stratospheric analyses during northern and southern winter. *J. Geophys. Res.,* **101,** 10 311–10 334.

Nash, J., and G. F. Forrester, 1986: Long-term monitoring of stratospheric temperature trends using radiance measurements obtained by the TIROS-N series of NOAA spacecraft. *Adv. Space Res.,* **6,** 37–44.

Naujokat, B., 1986: An update of the observed quasi-biennial oscillation of the stratospheric winds over the Tropics. *J. Atmos. Sci.,* **43,** 1873–1877.

Oort, A. H., 1983: Global atmospheric circulation statistics, 1958–1973. NOAA Professional Paper 14, 180 pp.

Pawson, S., and M. Fiorino, 1998a: A comparison of reanalyses in the tropical stratosphere. Part 1: Thermal structure and the annual cycle. *Climate Dyn.,* **14,** 631–644.

Pawson, S., and M. Fiorino, 1998b: A comparison of reanalyses in the tropical stratosphere. Part 2: The quasi-biennial oscillation. *Climate Dyn.,* **14,** 645–658.

Pawson, S., and Coauthors, 2000: The GCM-reality intercomparison project for SPARC (GRIPS): Scientific issues and initial results. *Bull. Amer. Meteor. Soc.,* **81,** 781–796.

Ramaswamy, V., and Coauthors, 2001: Stratospheric temperature trends: Observations and model simulations. *Rev. Geophys.,* **39,** 71–122.

Randel, W. J., 1987: The evaluation of winds from geopotential height data in the stratosphere. *J. Atmos. Sci.,* **44,** 3097–3120.

——, 1992: Global atmospheric circulation statistics, 1000-1 mb. NCAR Tech. Note NCAR/TN-366 STR, 256 pp.

——, and F. Wu, 1999: Cooling of the Arctic and Antarctic polar stratospheres due to ozone depletion. *J. Climate,* **12,** 1467–1479.

Remsberg, E. E., and Coauthors, 2002: An assessment of the quality

of HALOE temperature profiles in the mesosphere based on comparisons with Rayleigh backscatter lidar and inflatable falling sphere measurements. *J. Geophys. Res.,* **107**, 4447, doi: 10.1029/2001JD001521.

Russell, J. M., and Coauthors, 1993: The Halogen Occulation Experiment. *J. Geophys. Res.,* **98,** 10 777–10 979.

Scaife, A. A., J. Austin, N. Butchart, S. Pawson, M. Keil, J. Nash, and I. N. James, 2000: Seasonal and interannual variability of the stratosphere diagnosed from UKMO TOVS analyses. *Quart. J. Roy. Meteor. Soc.,* **126,** 2585–2604.

Smith, W. L., H. M. Woolf, C. M. Haydex, D. Q. Wark, and L. W. McMillin, 1979: The TIROS-N operational vertical sounder. *Bull. Amer. Meteor. Soc.,* **60,** 1177–1187.

SPARC, 2002: SPARC Intercomparison of Middle Atmosphere Climatologies. SPARC Rep. 3, 96 pp.

Swinbank, R., and A. O'Neill, 1994: A stratosphere–troposphere data assimilation system. *Mon. Wea. Rev.,* **122,** 686–702.

——, and D. A. Ortland, 2003: Compilation of wind data for the Upper Atmosphere Research Satellite (UARS) Reference Atmosphere Project. *J. Geophys. Res.,* **108,** 4615, doi:10.1029/2002JD003135.

Trenberth, K. E., and D. P. Stepaniak, 2002: A pathological problem with NCEP reanalyses in the stratosphere. *J. Climate,* **15,** 690–695.

Wu, D. L., and Coauthors, 2002: Mesospheric temperatures from UARS MLS: Retrieval and validation. *J. Atmos. Sol.-Terr. Phys.,* **65,** 245–267.